

DOI: 10.1002/chem.201301398

cine-Substitution Reactions of Metallabenzenes: An Experimental and Computational Study

Tongdao Wang,^[a] Hong Zhang,^[a, b] Feifei Han,^[a] Lipeng Long,^[a] Zhenyang Lin,^{*,[b]} and Haiping Xia^{*,[a]}

Abstract: Alkali-resistant osmabenzene [(SCN)₂(PPh₃)₂Os{CHC(PPh₃)CHCl-CH}] (**2**) can undergo nucleophilic aromatic substitution with MeOH or EtOH to give *cine*-substitution products [(SCN)₂(PPh₃)₂Os{CHC(PPh₃)CH-CHCR}] (R = OMe (**3**), OEt(**4**)) in the presence of strong alkali. However, the reactions of compound **2** with various amines, such as *n*-butylamine and aniline, afford five-membered ring species, [(SCN)₂(PPh₃)₂Os{CH=C(PPh₃)CH=C-(CH=NHR')}]] (R' = *n*Bu(**8**), Ph(**9**)), in addition to the desired *cine*-substitution products, [(SCN)₂(PPh₃)₂Os{CHC(PPh₃)CHCHC(NHR')}]] (R' = *n*Bu(**6**), Ph(**7**)), under similar reaction conditions. The mechanisms of these reac-

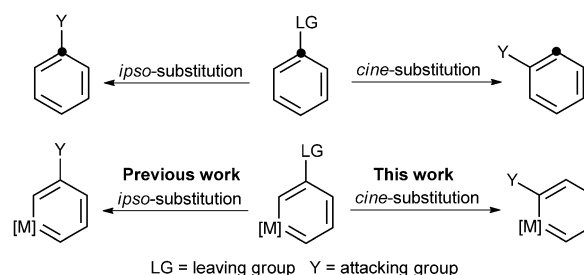
tions have been investigated in detail with the aid of isotopic labeling experiments and density functional theory (DFT) calculations. The results reveal that the *cine*-substitution reactions occur through nucleophilic addition, dissociation of the leaving group, protonation, and deprotonation steps, which resemble the classical "addition-of-nucleophile, ring-opening, ring-closure" (ANRORC) mechanism. DFT calculations suggest that, in the reac-

tion with MeOH, the formation of a five-membered metallacycle species is both kinetically and thermodynamically less favorable, which is consistent with the experimental results that only the *cine*-substitution product is observed. For the analogous reaction with *n*-butylamine, the pathway for the formation of the *cine*-substitution product is kinetically less favorable than the pathway for the formation of a five-membered ring species, but is much more thermodynamically favorable, again consistent with the experimental conversion of compound **8** into compound **6**, which is observed in an in situ NMR experiment with an isolated pure sample of **8**.

Keywords: aromaticity • *cine*-substitution • metallacycles • nucleophilic substitution • synthetic methods

Introduction

Aromatic substitution reactions are among the most widely and frequently used transformations in organic synthesis.^[1] Most studies in this field have concerned *ipso*-substitution, in which a new substituent is introduced at the same ring position as the departing leaving group (Scheme 1). In comparison with *ipso*-substitution, other patterns of aromatic substitution, for example, the *cine*-substitution of aromatic compounds is much less common.^[2] In *cine*-substitution re-



Scheme 1. Examples of substitution reactions in aromatic systems.

[a] T. Wang,^{*} Dr. H. Zhang,^{*} F. Han, L. Long, Prof. Dr. H. Xia
State Key Laboratory of Physical Chemistry of
Solid Surfaces, Collaborative Innovation Center of
Chemistry for Energy Materials, and
College of Chemistry and Chemical Engineering
Xiamen University, Xiamen, 361005 (P.R. China)
E-mail: hpxia@xmu.edu.cn

[b] Dr. H. Zhang,^{*} Prof. Dr. Z. Lin
Department of Chemistry
The Hong Kong University of Science and Technology
Clear Water Bay, Kowloon (Hong Kong)
E-mail: chzlin@ust.hk

[*] These authors contributed equally to this work.

Supporting information for this article is available on the WWW
under <http://dx.doi.org/10.1002/chem.201301398>.

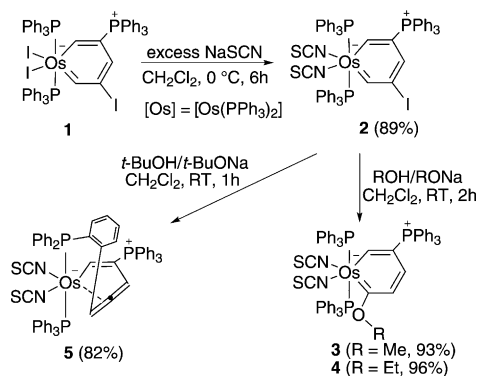
actions, the newly entering group takes up a position adjacent to that previously occupied by the leaving group.

As new aromatic heterocycles, metalla-aromatic compounds are currently attracting considerable attention, owing to their unique properties and promising applications.^[3] Extensive studies have been carried out on characteristic chemical reactions of metalla-aromatic compounds, such as electrophilic aromatic substitution (S_EAr)^[4] and nucleophilic aromatic substitution (S_NAr)^[5] reactions, which have provided strong evidence for the aromaticity of these aromatic heterocycles and have allowed us to obtain new interesting organometallic complexes. Until now, the reported

substitution reactions of metalla-aromatic compounds have been limited to *ipso*-substitution reactions. Given our long-standing interest in metallabenzene chemistry,^[5a-c,e,6] we investigated the nucleophilic reactions of metallabenzene complexes that contained an electron-withdrawing substituent and observed the first examples of *cine*-substitution for metalla-aromatic compounds. Herein, we report our experimental findings and, at the same time, provide our detailed DFT calculations on the reaction mechanism.

Results and Discussion

Reactions of osmabenzene complex [Os{CHC(PPh₃)CHCICH}(SCN)₂(PPh₃)₂] (2) with alcohols: Previously, we reported the synthesis of osmabenzene complex 1.^[6] Although osmabenzene complex 1 is stable in the solid state, it slowly decomposes in solution in the presence of alkali. Hence, we first modified this less-alkali-resistant osmabenzene complex through a ligand-substitution reaction. The treatment of compound 1 with six equivalents of sodium thiocyanate in CH₂Cl₂ led to the formation of the corresponding osmabenzene complex (2, Scheme 2). Osmabenzene complex 2 has been characterized by using multinuclear NMR spectroscopy and by single-crystal X-ray diffraction analysis, as well as by high-resolution mass spectroscopy. In the ¹H NMR spectrum, the two downfield signals of the OsCH protons appear at δ = 19.5 and 17.5 ppm. The ³¹P{¹H} NMR spectrum shows two singlet peaks at δ = -2.3 (OsPPh₃) and 19.0 ppm (CPPh₃). On the basis of ¹³C{¹H} NMR, ¹H, ¹³C HMQC, and ¹³C dept-135 NMR experiments, the five carbon signals of the metallacycle are identified at δ = 229.4 (C1), 112.7 (C2), 154.0 (C3), 97.4 (C4), and 261.5 ppm (C5).



Scheme 2. Preparation of osmabenzene 2 and the reactions of compound 2 with alcohols.

The crystallographic details of osmabenzene complex 2 are listed in Table 3; selected bond lengths and angles are listed in Table 1. As shown in Figure 1, osmabenzene complex 2 contains an essentially planar metallabenzene unit. The C–C bond lengths in the C1–C5 chain are within the

Table 1. Selected bond lengths and angles in compounds 2, 3, and 5.

	2	3	5
Bond length [Å]			
Os1–C1	1.982(6)	1.980(7)	2.031(6)
Os1–C5	1.939(8)	1.953(9)	2.202(6)
Os1–C4			2.037(6)
C1–C2	1.377(9)	1.395(12)	1.365(7)
C2–C3	1.426(10)	1.421(13)	1.466(8)
C3–C4	1.369(10)	1.325(14)	1.344(8)
C4–C5	1.406(11)	1.411(15)	1.400(8)
Bond angle [°]			
C5–Os1–C1	89.9(3)	90.3(4)	111.0(2)
C1–Os1–C4			72.7(2)
C2–C1–Os1	128.1(5)	127.7(6)	122.0(4)
C1–C2–C3	123.9(6)	121.9(8)	112.0(5)
C4–C3–C2	123.8(7)	128.1(11)	108.8(5)
C3–C4–C5	124.8(7)	123.0(11)	158.2(6)
C4–C5–Os1	128.4(5)	128.5(9)	64.5(3)
C3–C4–Os1			124.6(5)

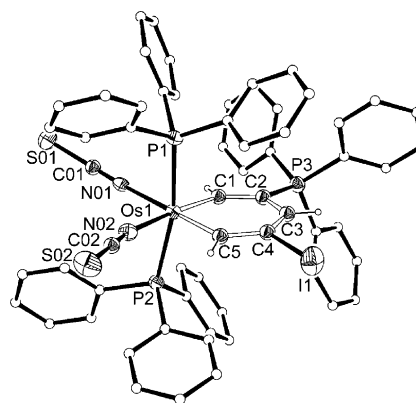


Figure 1. Molecular structure of compound 2. Ellipsoids set at 50% probability. The hydrogen atoms of the PPh₃ groups are omitted for clarity.

range 1.369(10)–1.426(10) Å and the lack of significant alterations in the C–C bond lengths suggests that compound 2 has a delocalized structure.

Osmabenzene complex 2 can tolerate strong bases in solution. When an excess of sodium methoxide was added as a solution in MeOH to the solution of compound 2 in CH₂Cl₂, the reaction yielded a new osmabenzene complex (3), which was a product of a *cine*-substitution reaction, within 2 h at room temperature (Scheme 2). This new osmabenzene complex (3) was isolated as greenish solid in 93% yield. The crystal structure of compound 3 has been determined and its molecular structure is shown in Figure 2, which confirms that the methoxy group is attached onto the C5 atom of the essentially planar osmabenzene ring. All of the bond lengths of the metallacycle fall within the observed range for other typical metallabenzene complexes.^[3] The two Os–C bond lengths are almost equal (Os–C1 1.980(7) and Os–C5 1.953(9) Å) and the ring C–C distances are consistent with delocalization (C1–C2 1.395(12), C2–C3 1.421(13), C3–C4 1.325(14), and C4–C5 1.411(15) Å). The change in the substituents on the metallacyclic ring is also clearly evident by NMR spectroscopy. In particular, the ¹H NMR (CDCl₃) spectrum shows

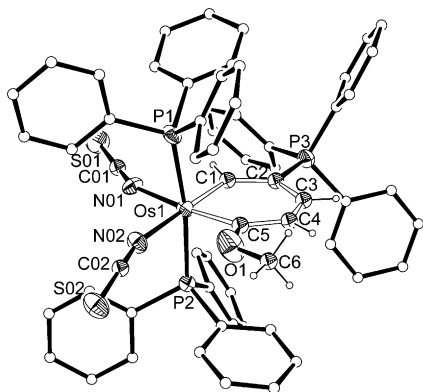


Figure 2. Molecular structure of compound **3**. Ellipsoids set at 50% probability. The hydrogen atoms of the PPh₃ groups are omitted for clarity.

three ¹H signals of the metallabenzene ring at $\delta=16.0$ (C1H), 7.1 (C3H), and 5.5 ppm (C4H). With the aid of ¹H,¹³C HSQC and ¹³C dept-135 NMR experiments, the five carbon signals of the metallabenzene ring are observed at $\delta=234.4$ (C1), 102.2 (C2), 146.1 (C3), 114.6 (C4), and 249.7 ppm (C5) in the ¹³C{¹H} NMR spectrum. The presence of a methoxy substituent is evident by the chemical shifts in the ¹H NMR ($\delta=2.8$ ppm) and ¹³C{¹H} NMR spectra ($\delta=57.5$ ppm).

The reactions of osmabenzene complex **2** with other alcohol nucleophiles were also investigated. Compound **2** reacted with EtOH to produce *cine*-substitution product **4** in the presence of sodium ethoxide (Scheme 2). Compound **4** was characterized by NMR spectroscopy and by high-resolution mass spectroscopy. The structure of compound **4** can be easily deduced, because its NMR data are similar to those of osmabenzene complex **3**. The resonances of the osmabenzene ring in the ¹H NMR ($\delta=16.1$ (C1H), 7.2 (C3H), and 5.6 ppm (C4H)) and ¹³C{¹H} NMR spectra ($\delta=234.7$ (C1), 102.1 (C2), 146.3 (C3), 113.8 (C4), and 248.8 ppm (C5)) are very close to those that were observed for osmabenzene complex **3**. The ethoxy substituent is readily distinguished in the ¹H NMR ($\delta=3.0$ (C6H) and 0.7 ppm (C7H)) and ¹³C{¹H} NMR spectra ($\delta=65.6$ (C6) and 14.8 ppm (C7)).

Notably, the reaction of osmabenzene complex **2** with the bulky *tert*-butanol in the presence of sodium *tert*-butoxide did not give the desired *cine*-substitution product. Instead, as shown in Scheme 2, allene-coordinated complex **5** was isolated from the reaction. The structure of compound **5** has been determined by using X-ray crystallography, as shown in Figure 3. The X-ray diffraction study confirmed that the complex contained a conjugated osmacycle, as well as a terminal double bond from an allene that was coordinated to the metal center. As a consequence of its coordination to the metal center and because one of its substituents is part of a phosphine ligand, the allene unit is strongly bent, with a C3-C4-C5 angle of 158.2(6)°. In addition, the characteristic spectroscopic data of compound **5** are also consistent with an allene-coordinated osmacyclic structure. The ¹H NMR spectrum shows the signals of the metallacycle at $\delta=11.2$

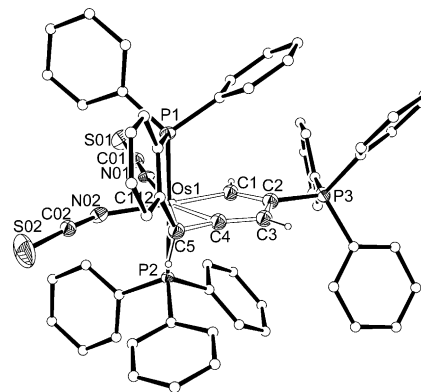
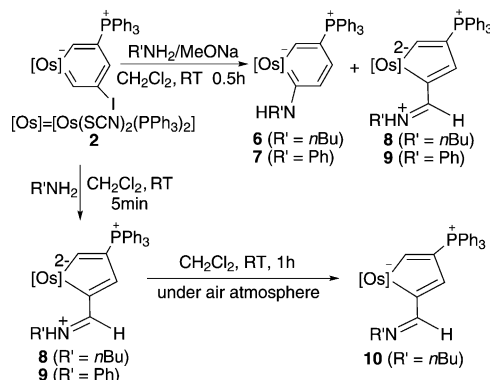


Figure 3. Molecular structure of compound **5**. Ellipsoids set at 50% probability. The hydrogen atoms of the PPh₃ groups are omitted for clarity.

(C1H), 7.0 (C3H), and 3.8 ppm (C5H). In the ³¹P{¹H} NMR spectrum, the signal of the CPh₃ atom appears at $\delta=9.3$ ppm and the signals of the two phosphine ligands are observed at $\delta=16.0$ (OsPPh₂(C₆H₅)CH) and -3.5 ppm (OsPPh₃). In the ¹³C{¹H} NMR spectrum, the signals of the C1 and C2 atoms appear at $\delta=207.3$ and 116.1 ppm, whereas the three carbon signals of the coordinated allene backbone appear at $\delta=126.0$ (C3), 199.7 (C4), and 49.9 ppm (C5).

Reactions of osmabenzene complex **2 with amines:** To study the scope of these *cine*-substitution reactions, the reaction of osmabenzene complex **2** with *n*-butylamine was first investigated. The reaction was monitored by in situ NMR spectroscopy. When a solution of sodium methoxide in MeOH was added to a solution of compound **2** and excess *n*-butylamine in CH₂Cl₂, compound **2** was completely consumed to give a 2:3 mixture of complexes **6** and **8** within 30 min (Scheme 3). Complex **6** can be isolated as a green solid from the reaction mixture because of its good solubility in Et₂O (complex **8** is insoluble in Et₂O). Similar to those of compounds **3** and **4**, the ¹H NMR ($\delta=15.2$ (C1H), 6.8 (C3H), and 5.4 ppm (C4H)) and ¹³C{¹H} NMR spectra ($\delta=212.7$ (C1), 101.4 (C2), 143.4 (C3), 112.1 (C4), and 229.7 ppm (C5)) for the



Scheme 3. Reactions of osmabenzene **2** with amines.

metallacycle atoms of complex **6** confirm that complex **6** is a *cine*-substitution product and that substitution occurs at the C5 position. The resonances of the *n*-butylamine group are observed in the ^1H NMR ($\delta=2.0$ (C6H), 0.6 (C7H), 0.9 (C8H), and 0.6 ppm (C9H)) and $^{13}\text{C}\{^1\text{H}\}$ NMR spectra ($\delta=45.5$ (C6), 30.9 (C7), 20.4 (C8), and 14.2 ppm (C9)).

Owing to its high sensitivity to air and its poor solubility in ordinary organic solvents, our attempts to perform a full NMR spectroscopic characterization of complex **8** failed. However, the structure of compound **8** could still be deduced from its ^1H NMR and $^{31}\text{P}\{^1\text{H}\}$ NMR spectra. In addition, high-resolution mass spectroscopy of complex **8** showed a peak at m/z 1229.2903, which was consistent with the supposed formula. Besides, we obtained the oxidation product of compound **8**, a complex that was structurally similar to complex **8** (see below).

By using different amines, such as aniline, as the nucleophile, we carried out analogous reactions and observed similar results. The reaction produced the expected *cine*-substitution product (**7**) and the five-membered ring product (**9**) in a molar ratio of 5:6. These complexes have also been characterized by using NMR spectroscopy and by high-resolution mass spectroscopy. For compound **7**, the resonances of the ring atoms in the ^1H NMR ($\delta=15.3$ (OsCH), 6.9 (C3H), and 6.0 ppm (C4H)) and $^{13}\text{C}\{^1\text{H}\}$ NMR spectra ($\delta=217.3$ (C1), 102.4 (C2), 143.2 (C3), 115.2 (C4), and 228.9 ppm (C5)) are comparable to those for compounds **3**, **4** and **6**, which are all in accord with the osmabenzene structure with a phenylamino substituent that is attached onto the C5 position. There are only a few examples of metallabenzenes that contain electron-donating groups on the metallacycle.^[4e,5d,6q,7] Thus, complexes **6** and **7** represent unprecedented amino-substituted metallabenzenes.

We noted that only *cine*-substitution products were obtained from the reactions of compound **2** with alcohols in the presence of sodium methoxide. However, the reactions of compound **2** with amines in presence of sodium methoxide not only produced *cine*-substitution products but also the five-membered ring products. Because amines are typically more nucleophilic/basic than their alcohol equivalents, we postulated that the five-membered ring products may be formed through the direct reactions between compound **2** and amines without the aid of a strong alkali. To test this idea, we performed the reaction of compound **2** with *n*-butylamine in the absence of sodium methoxide. Indeed, when excess *n*-butylamine was added to the solution of compound **2** in CH_2Cl_2 , it was completely converted into complex **8** within five minutes (Scheme 3).

When a solution of complex **8** was stirred at room temperature in air for one hour, it was cleanly converted into paramagnetic complex **10** (Scheme 3). Complex **10** was isolated as green solid and characterized by single-crystal X-ray diffraction analysis and by high-resolution mass spectroscopy. The crystallographic details are given in Table 3 and selected bond lengths and angles are given in Table 2. The molecular structure of the complex is shown in Figure 4. X-ray diffraction analysis indicates that compound **10** contains a metalla-

Table 2. Selected bond lengths and angles in compound **10**.

Bond length [Å]			
Os1–C1	1.977(2)	C5–N1	1.306(3)
Os1–C4	2.082(2)	N1–C6	1.467(3)
C1–C2	1.395(3)	C6–C7	1.518(4)
C2–C3	1.423(3)	C7–C8	1.519(4)
C3–C4	1.390(3)	C8–C9	1.518(5)
C4–C5	1.413(3)		
Bond angle [°]			
C4–Os1–C1	77.96(9)	C4–C3–C2	115.1(2)
C2–C1–Os1	119.37(16)	C3–C4–Os1	114.69(16)
C1–C2–C3	112.8(2)		

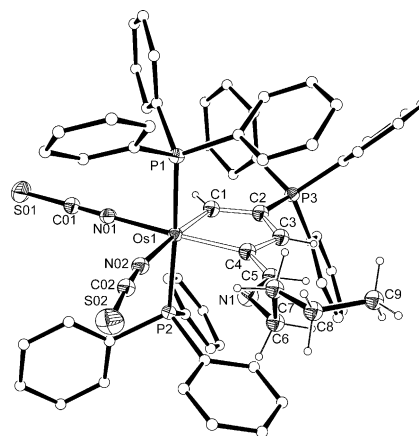


Figure 4. Molecular structure of compound **10**. Ellipsoids set at 50% probability. The hydrogen atoms of the PPh_3 groups are omitted for clarity.

cyclopentadiene ring with an exocyclic imino group. Complexes **8** and **10** have similar overall structural features, despite the fact that they have different electron counts. Clearly, complex **8** is easily oxidized in air to generate the oxidation product (**10**). Similar results were observed when aniline was allowed to react with osmabenzene complex **2** in the absence of sodium methoxide (Scheme 3).

Mechanistic investigation of the reactions of compound **2** with various nucleophiles:

To understand the mechanistic aspects of the reactions of compound **2** with various nucleophiles, we initially performed the same experiments starting from deuterium-labeled MeOH. As shown in Scheme 4, the experiments suggest that the hydrogen atom at the C4 position in the *cine*-substitution product comes from the MeOH proton. Interestingly, with $\text{CD}_3\text{OD}/\text{MeONa}$, CD_3O (instead of MeO) and D were found at the C5 and C4 positions, re-



Scheme 4. Reactions of osmabenzene **2** with deuterium-labeled MeOH.

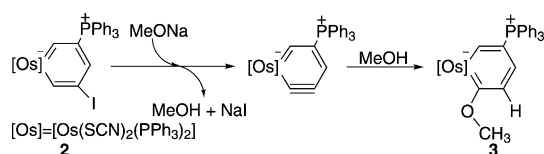
Table 3. Crystal data and structure refinement for compounds **2**, **3**, **5**, and **10**.

	2 ·2.5 CHCl ₃	3 ·CH ₂ Cl ₂	5 ·2CH ₂ Cl ₂	10 ·2CHCl ₂
formula	C _{63.50} H _{50.50} N ₂ S ₂ P ₃ ICl _{7.50} Os	C ₆₃ H ₅₃ N ₂ S ₂ P ₃ Cl ₂ OOS	C ₆₃ H ₅₁ N ₂ S ₂ P ₃ Cl ₄ Os	C ₆₇ H ₆₁ N ₃ S ₂ P ₃ Cl ₄ Os
M _w	1581.56	1272.20	1325.09	1397.22
T [K]	173	173	123	173
λ [Å] (MoK _α or CuK _α radiation)	0.71073	0.71073	0.71073	1.54178
crystal system	monoclinic	monoclinic	orthorhombic	monoclinic
space group	P21/c	P21/n	Pbca	P21/c
a [Å]	23.123(3)	12.739(2)	14.9224(4)	21.91400(10)
b [Å]	12.8492(17)	19.773(4)	17.7297(6)	12.38410(10)
c [Å]	25.086(3)	22.575(4)	43.1777(15)	23.4976(2)
α [°]	90	90	90	90
β [°]	117.423(2)	96.992(3)	90	103.8430(10)
γ [°]	90	90	90	90
V [Å ³]	6615.8(15)	5644.2(17)	11423.5(6)	6191.68(8)
Z	4	4	8	4
ρ _{calcd} [g cm ⁻³]	1.588	1.497	1.541	1.499
μ [mm ⁻¹]	2.873	2.557	2.619	7.179
F(000)	3116	2560	5312	2820
crystal size [mm ³]	0.20 × 0.20 × 0.10	0.30 × 0.20 × 0.20	0.20 × 0.20 × 0.10	0.20 × 0.10 × 0.04
θ range [°]	0.99–25.00	1.37–25.00	2.73–25.00	3.87–60.16
total reflns	33 015	28 388	27 875	34 268
unique reflns	11 655	9912	10 050	9218
observed reflns	9805	9190	6066	8759
[I ≥ 2σ(I)]				
data/restraints/parameters	11655/135/776	9912/54/655	10050/0/676	9218/0/721
GOF on F ²	1.000	1.000	0.867	1.000
R ₁ /wR ₂ [I ≥ 2σ(I)]	0.0507/0.1476	0.0663/0.1858	0.0437/0.0767	0.0201/0.0491
R ₁ /wR ₂ (all data)	0.0606/0.1531	0.0719/0.1915	0.0866/0.0833	0.0217/0.0500
largest peak/hole [e Å ⁻³]	2.219/−1.280	2.144/−2.159	1.084/−2.480	0.694/−0.884
CCDC No. ^[a]	920029	920030	920031	920028

[a] These files contain the supplementary crystallographic data for this paper. These data can be obtained free of charge from The Cambridge Crystallographic Data Centre via www.ccdc.cam.ac.uk/data_request/cif.

spectively, in the *cine*-substitution product. The isotopic-labeling experiments suggest that the nucleophilic attack of MeOH, not MeONa, on the metallabenzene ring initiates the reaction, owing to the poor solubility of sodium methoxide in the reaction mixture and to the relatively dominant amount of MeOH (about 60 equiv with respect to MeONa). For more details on the isotope-labeling experiments, see the Supporting Information.

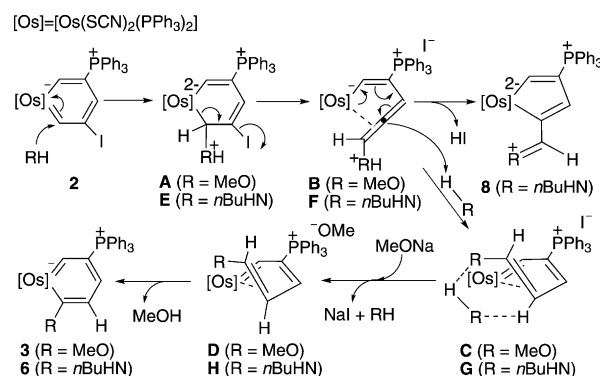
Thus, we first attempted to see whether we could find further support for the mechanism of this *cine*-substitution reaction, which was proposed to involve an elimination/addition process through a metallabenzynes intermediate (Scheme 5). The proposed elimination/addition mechanism is similar to the classical examples of *cine*-substitution, which proceed through benzyne intermediates in homoarene



Scheme 5. Proposed elimination-addition mechanism for the reaction of osmabenzene **2** with MeOH.

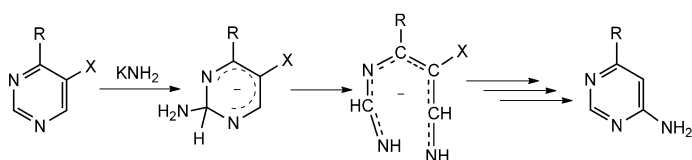
derivatives. However, our attempts to trap the possible metallabenzynes intermediate by performing a [4+2] cycloaddition reaction with furan or pyrrole failed. Successful trapping is generally believed to be strong supporting evidence for the existence of a benzyne-type intermediate.

As mentioned above, *cine*-substitution does not occur for the reactions of osmabenzene complex **2** with alcohols or amines in the absence of strong alkali. Furthermore, the direct reactions of compound **2** with amines only afford five-membered ring products **8** or **9**. Taking these observations into account, we can consider a plausible mechanism (Scheme 6) that is supported by our DFT calculations (see below). The nucleophilic addition of a molecule of MeOH (or *n*-butylamine) at the C5 position results in the formation of σ^H adduct **A** (or **E**). Then, dissociation of the halide anion affords allene-coordinated in-



Scheme 6. Proposed mechanism for the reactions of osmabenzene **2** with nucleophiles.

intermediate **B** (or **F**). The attack of a proton from another nucleophile onto the central carbon atom of the allene moiety of structure **B** (or **F**) induces redistribution of the π-conjugation system and produces alkene-coordinated intermediate **C** (or **G**). Subsequent replacement of the counteranion by sodium methoxide and the dissociation of a molecule of MeOH or *n*-butylamine may produce intermediate **D** (or **H**). Finally, deprotonation of the C5–H bond yields



Scheme 7. Amination of pyrimidine derivatives (ANRORC mechanism).

osmabenzene **3** (or **6**). The whole process, as presented in Scheme 6, resembles the classical ANRORC mechanism (Scheme 7), which has been thoroughly investigated by van de Plas and co-workers,^[8] thereby proceeding through a sequence that comprises three key steps: 1) the addition of the nucleophile, 2) ring opening, and 3) ring closure. In the absence of strong alkali, five-membered ring product **8** is exclusively formed (**2**→**E**→**F**→**8**).

DFT studies: As mentioned above, our DFT calculations support the mechanisms proposed in Scheme 6. In this section, the results of the DFT calculations will be given and discussed in detail. From these DFT results, we also want to understand the experimental observations that the reactions of compound **2** with amines also produced five-membered ring products with the desired *cine*-substitution product, whereas the *cine*-substitution products were exclusively formed from the reactions of compound **2** with alcohols.

Figure 5 shows the calculated energy profile based on the mechanism shown in Scheme 6, which leads to the formation of experimentally observed *cine*-substitution product **3**. In Figure 5, the labels of the model compounds are followed by the prime (') symbol to differentiate them from their corresponding experimental compounds.

Scheme 6 shows that the nucleophilic attack of a molecule of MeOH onto the C5 position of compound **2** is followed by the dissociation of iodide, which initiates the reaction to lead to the formation of allene-coordinated complex **B**. Interestingly, the calculations indicate that this event is a one-

step process (Figure 5). As shown in Figure 5, allene-coordinated complex **B'** is directly formed from compound **2** and MeOH through transition state **TSB**, with a barrier of 27.2 kcal mol⁻¹. From structure **B'**, there are two possible paths, that is, paths **a** and **b**, which lead to the formation of the expected *cine*-substitution product and the five-membered ring species (which are only observed in the reactions with amines), respectively. In path **a**, the electrophilic addition of another molecule of MeOH through the attack of a proton onto the central carbon of the allene moiety of structure **B'** proceeds through six-membered transition state **TSC1** to give intermediate **C'**. This addition step is a fast process with a small barrier (3.2 kcal mol⁻¹). Structure **C'** is an ion-pair species that can mix well with the base (MeONa) in solution and facilitate further reaction. Then, ion exchange of MeO⁻ for I⁻ take place, followed by deprotonation at the C5 position, thereby giving intermediate **D1'** with a barrier of 14.9 kcal mol⁻¹. Finally, the formation of a bond between the C5 position and the metal center, accompanied with aromatization, generates *cine*-substitution product **3'**. The rate-determining step for the whole reaction corresponds to the first addition of MeOH, followed by iodide dissociation, with a calculated barrier of 27.2 kcal mol⁻¹.

In path **b**, which leads to the formation of the five-membered metallacyclic species, the elimination of HI from structure **B'** occurs to first give structure **B2'**. Then, structural rearrangement generates five-membered metallacycle species **C2'**. Figure 5 shows that path **b** is less favorable than path **a**. Furthermore, osmacyclopentadiene complex **C2'** is relatively unstable. The instability of structure **C2'** can be attributed to its highly reactive oxonium structure. Therefore, the formation of the five-membered metallacycle species in the reaction with MeOH is kinetically and thermodynamically less favorable, consistent with the experimental results for the reaction of compound **2** with MeOH in the presence of sodium methoxide, which affords the net *cine*-substitution product.

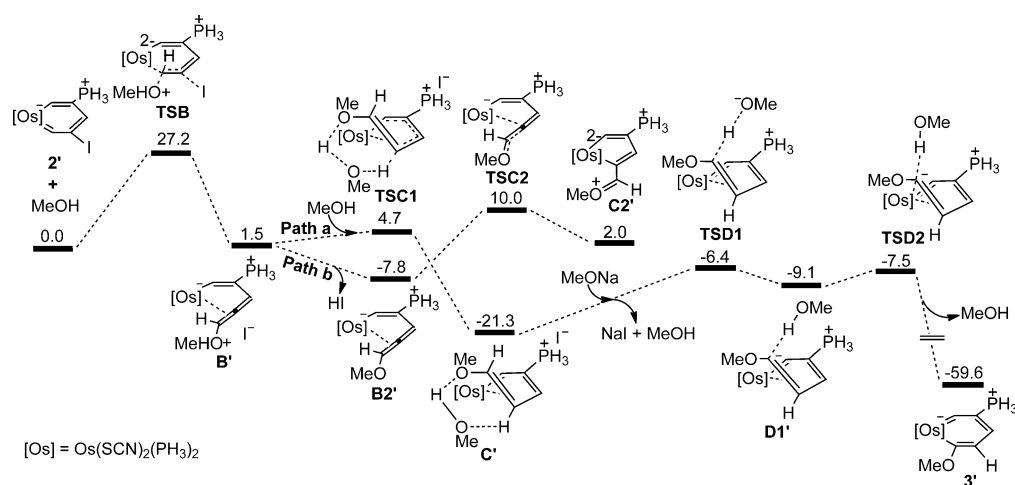


Figure 5. Calculated energy profile for the formation of structure **3'**, based on the reaction mechanism shown in Scheme 6. The relative electronic energies are given in kcal mol⁻¹.

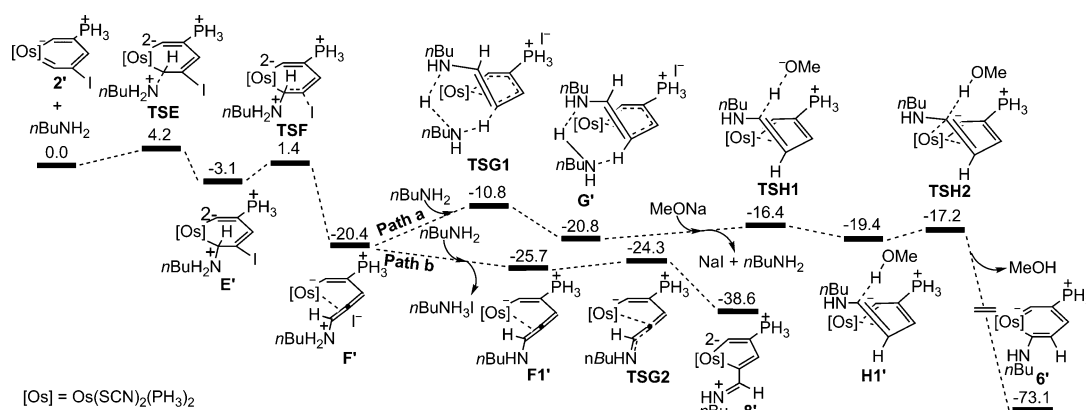


Figure 6. Calculated electronic energy profile for the formation of structures **6'** and **8'**, based on the reaction mechanism shown in Scheme 6. The relative electronic energies are given in kcal mol⁻¹.

We also calculated the reaction of metallabenzene complex **2** with *n*-butylamine. Figure 6 shows the calculated energy profile for the mechanism presented in Scheme 6. Nucleophilic addition of an amine molecule and dissociation of the halide anion afford allene-coordinated intermediate **F'**. Unlike the reaction with MeOH, the event that leads to the formation of allene-coordinated intermediate **F'** is a two-step process, which may be attributed to the higher stability of iminium ion intermediate **E'** compared to that of the analogous oxonium ion intermediate. In addition, the barrier to the addition is much lower than the corresponding one in the reaction with MeOH, in agreement with the experimental observations that the reaction time with *n*-butylamine is significantly shorter than that with MeOH. All of these results indicate that *n*-butylamine is a much-stronger nucleophile than MeOH in these reactions.

From structure **F'**, there are again two paths, that is, paths **a** and **b**, thus leading to the formation of the *cine*-substitution product and the five-membered ring product, respectively. Because of the greater nucleophilicity of *n*-butylamine, path **b**, which involves the elimination of HI and a structural rearrangement to give five-membered ring product **8'**, is kinetically very favorable. In addition, five-membered ring product **8'** is more stable than intermediate **F'**. Consistent with this theoretical result, five-membered ring product **8** was observed (and characterized) experimentally.

The calculated energy profile (Figure 6) for path **a**, which leads to the formation of the *cine*-substitution product, is similar to the profile for the reaction with MeOH (Figure 5). The results of the calculations (Figure 6) indicate that this pathway is kinetically less favorable than path **b**, but is much more thermodynamically favorable.

Comparing the calculated energy profiles for the two pathways, we can conclude that structure **8'** is a kinetic product whilst structure **6'** is the thermodynamic product and that structure **8'** can be converted into structure **6'** because the barrier for the conversion is accessible (27.8 kcal mol⁻¹, which corresponds to the energy difference between structure **8'** and **TSG1**; Figure 6).

Prompted by the results of the calculations discussed above, we isolated a pure sample of compound **8** and, by performing in situ NMR experiments, we observed that it could be converted into *cine*-substitution product **6** in solution in the presence of excess *n*-butylamine, hydriodic acid, and sodium methoxide.

Conclusion

In summary, the first examples of *cine*-substitution reactions of metalla-aromatic compounds have been observed experimentally and studied computationally. The net *cine*-substitution products can be obtained from the reactions of osma-benzene with alcohols in the presence of strong alkali. For the reactions with amines, the desired *cine*-substitution products can also be achieved, together with the five-membered ring species under similar reaction conditions. All of our investigations (i.e., in situ NMR experiments and isotopic labeling experiments) support the conclusion that *cine*-substitution reactions involve a sequence of three key steps: the addition of a nucleophile, ring opening, and ring closure, which resemble the classical ANRORC mechanism. These findings were corroborated by using DFT calculations and demonstrate that the nucleophilicity of the nucleophiles and the basicity of the reaction conditions are crucial for *cine*-substitution reactions.

Experimental Section

General comments: All manipulations were carried out at room temperature under a nitrogen atmosphere by using standard Schlenk techniques, unless otherwise stated. Solvents were distilled under a nitrogen atmosphere from sodium benzophenone (Et₂O, *n*-hexane) or calcium hydride (CH₂Cl₂). Column chromatography was performed on neutral alumina gel (200–300 mesh). The starting material [I₂(PPh₃)₂Os{CHC(PPh₃)CHCICH}] (**1**) was synthesized according to a literature procedure.^[61] NMR experiments were performed on Bruker AV-500 (¹H: 500.2 MHz, ¹³C: 125.8 MHz, ³¹P: 202.5 MHz) or Bruker AV-400 spectrometers (¹H: 400.1 MHz, ¹³C: 100.6 MHz, ³¹P: 162.0 MHz). ¹H and

^{13}C NMR chemical shifts are reported relative to TMS; ^{31}P NMR chemical shifts are reported relative to 85% H_3PO_4 . High-resolution mass spectra (HRMS) were recorded on a Bruker En Apex Ultra 7.0T FTMS mass spectrometer.

Synthesis of [(SCN) $_2$ (PPh $_3$) $_2$ Os{CHC(PPh $_3$)CHCICH}] (2): A mixture of compound **1** (460 mg, 0.32 mmol) and sodium thiocyanate (158 mg, 1.95 mmol) in CH_2Cl_2 (35 mL) was stirred at 0°C for about 6 h to give a green suspension. The solvent was removed under vacuum and the residue was extracted with CH_2Cl_2 (3 \times 5 mL). The volume of the filtrate was concentrated to about 5 mL under vacuum; the addition of Et_2O (50 mL) to the solution produced a green solid, which was collected by filtration, washed with Et_2O (3 \times 5 mL), and dried under vacuum. Yield: 370 mg, 89%; ^1H NMR (500.2 MHz, CDCl_3): δ = 19.5 (s, 1H; C^5H), 17.5 (d, $J(\text{P,H})$ = 21.6, 1H; C^1H), 8.0 (d, $J(\text{P,H})$ = 12.2 Hz, 1H; C^3H), 6.8–7.7 ppm (m, 45H; Ph); $^{31}\text{P}\{^1\text{H}\}$ NMR (202.5 MHz, CDCl_3): δ = 19.0 (s; C^2PPh_3), –2.3 ppm (s; OsPPh_3); $^{13}\text{C}\{^1\text{H}\}$ NMR (125.8 MHz, CDCl_3 , with $^1\text{H},^{13}\text{C}$ HSQC and ^{13}C dept-135 NMR experiments): δ = 229.4 (br; C^1), 261.5 (br; C^5), 154.0 (d, $J(\text{P,C})$ = 21.9 Hz; C^3), 146.9 and 143.0 (s; $\text{Os}(\text{NCS})_2$), 134.4–120.6 (m; Ph), 112.7 (d, $J(\text{P,C})$ = 72.5 Hz; C^2), 97.4 ppm (d, $J(\text{P,C})$ = 14.1 Hz; C^4); HRMS (ESI): m/z calcd for $\text{C}_{61}\text{H}_{48}\text{N}_2\text{S}_2\text{P}_3\text{Os}$: 1284.1126 [M] $^+$; found: 1284.1108.

Synthesis of [(SCN) $_2$ (PPh $_3$) $_2$ Os{CHC(PPh $_3$)CHCHC(OMe)}] (3): A suspension of sodium methoxide (16 mg, 0.30 mmol) in MeOH (1 mL, 24.71 mmol) was added to a solution of compound **2** (120 mg, 0.09 mmol) in CH_2Cl_2 (10 mL). The mixture was stirred at RT for about 2 h to give a green suspension. The solvent was removed under vacuum and the residue was extracted with CH_2Cl_2 (3 \times 2 mL). The volume of the filtrate was concentrated to about 2 mL under vacuum; the addition of *n*-hexane (30 mL) to the solution produced a green solid that was collected by filtration, washed with *n*-hexane (3 \times 2 mL), and dried under vacuum. Yield: 103 mg, 93%; ^1H NMR (500.2 MHz, CDCl_3): δ = 16.0 (d, $J(\text{P,H})$ = 22.5 Hz, 1H; C^1H), 6.8–7.8 ppm (m, 45H; Ph), 7.1 (t, $J(\text{P,H})$ = 10.3 Hz, $J(\text{H,H})$ = 10.3 Hz, 1H; C^3H), obscured by the phenyl signals but confirmed by $^1\text{H},^{13}\text{C}$ HMQC experiments), 5.5 (d, $J(\text{H,H})$ = 10.3 Hz, 1H; C^4H), 2.8 ppm (s, 3H; OCH_3); $^{31}\text{P}\{^1\text{H}\}$ NMR (202.5 MHz, CDCl_3): δ = 17.0 (s; C^2PPh_3), –5.4 ppm (s; OsPPh_3); $^{13}\text{C}\{^1\text{H}\}$ NMR (125.8 MHz, CDCl_3 , with $^1\text{H},^{13}\text{C}$ HSQC and ^{13}C dept-135 NMR experiments): δ = 234.4 (br; C^1), 249.7 (br; C^5), 146.1 (d, $J(\text{P,C})$ = 22.5 Hz; C^3), 141.7 and 139.9 (s; $\text{Os}(\text{NCS})_2$), 139.9–114.5 (m; Ph), 114.6 (d, $J(\text{P,C})$ = 12.4 Hz; C^4), 102.2 (d, $J(\text{P,C})$ = 78.2 Hz; C^2), 57.5 ppm (s; OCH_3); HRMS (ESI): m/z calcd for $\text{C}_{60}\text{H}_{51}\text{N}_2\text{S}_2\text{P}_3\text{Os}$: 1188.2265 [M] $^+$; found: 1188.2264.

Synthesis of [(SCN) $_2$ (PPh $_3$) $_2$ Os{CHC(PPh $_3$)CHCHC(OEt)}] (4): A suspension of sodium ethoxide (21 mg, 0.31 mmol) in EtOH (1 mL, 17.13 mmol) was added to a solution of compound **2** (130 mg, 0.10 mmol) in CH_2Cl_2 (10 mL). The mixture was stirred at RT for about 2 h to give a green suspension. The solvent was removed under vacuum and the residue was extracted with CH_2Cl_2 (3 \times 2 mL). The volume of the filtrate was concentrated to about 2 mL under vacuum; the addition of *n*-hexane (30 mL) to the solution produced a green solid that was collected by filtration, washed with *n*-hexane (3 \times 2 mL), and dried under vacuum. Yield: 117 mg, 96%; ^1H NMR (500.2 MHz, CDCl_3): δ = 16.1 (d, $J(\text{P,H})$ = 22.5 Hz, 1H; C^1H), 6.8–7.8 ppm (m, 45H; Ph), 7.2 (t, $J(\text{P,H})$ = 10.2 Hz, $J(\text{H,H})$ = 10.2 Hz, 1H; C^3H), obscured by the phenyl signals but confirmed by $^1\text{H},^{13}\text{C}$ HMQC experiments), 5.6 (d, $J(\text{H,H})$ = 10.2 Hz, 1H; C^4H), 3.0 (q, $J(\text{H,H})$ = 6.5 Hz, 2H; OCH_2CH_3), 0.7 ppm (t, $J(\text{H,H})$ = 6.4 Hz, 3H; OCH_2CH_3); $^{31}\text{P}\{^1\text{H}\}$ NMR (202.5 MHz, CDCl_3): δ = 17.3 (s; C^2PPh_3), –4.9 ppm (s; OsPPh_3); $^{13}\text{C}\{^1\text{H}\}$ NMR (125.8 MHz, CDCl_3 , with $^1\text{H},^{13}\text{C}$ HSQC and ^{13}C dept-135 NMR experiments): δ = 234.7 (br; C^1), 248.8 (br; C^5), 146.3 (d, $J(\text{P,C})$ = 22.8 Hz; C^3), 141.3 and 139.6 (s; $\text{Os}(\text{NCS})_2$), 140.0–113.8 (m; Ph), 113.8 (d, $J(\text{P,C})$ = 12.6 Hz; C^4), 102.1 (d, $J(\text{P,C})$ = 78.0 Hz; C^2), 65.6 (s; OCH_2CH_3), 14.8 ppm (s; OCH_2CH_3); HRMS (ESI): m/z calcd for $\text{C}_{60}\text{H}_{53}\text{N}_2\text{S}_2\text{P}_3\text{Os}$: 1202.2427 [M] $^+$; found: 1202.2453.

Synthesis of [(SCN) $_2$ (PPh $_3$) $_2$ (PPh $_2$ (C_6H_4))Os{CHC(PPh $_3$)CH(η^2 -CCH)}] (5): A suspension of sodium *tert*-butoxide (82 mg, 0.85 mmol) in *tert*-butanol (1.5 mL, 15.68 mmol) was added to a solution of compound **2** (205 mg, 0.16 mmol) in CH_2Cl_2 (15 mL). The mixture was stirred at RT for about 1 h to give a yellow suspension. The solvent was removed

under vacuum and the residue was extracted with CH_2Cl_2 (3 \times 2 mL). The volume of the filtrate was concentrated to about 2 mL under vacuum; the addition of *n*-hexane (20 mL) to the solution produced a yellow solid that was collected by filtration, washed with *n*-hexane (3 \times 2 mL), and dried under vacuum. Yield: 151 mg, 82%; ^1H NMR (500.2 MHz, CD_2Cl_2): 11.2 (d, $J(\text{P,H})$ = 16.9 Hz, 1H; C^1H), 7.0 (d, $J(\text{P,H})$ = 6.9 Hz, 1H; C^3H), obscured by the phenyl signals but confirmed by $^1\text{H},^{13}\text{C}$ HMQC experiments), 6.7–7.7 (m, 44H; Ph), 3.8 ppm (s, 1H; C^5H); $^{31}\text{P}\{^1\text{H}\}$ NMR (202.5 MHz, CD_2Cl_2): δ = 9.3 (s; C^2PPh_3), 16.0 (d, $J(\text{P,P})$ = 302.0 Hz; $\text{OsPPh}_2(\text{C}_6\text{H}_4)\text{CH}$), –3.5 ppm (d, $J(\text{P,P})$ = 302.5 Hz; OsPPh_3); $^{13}\text{C}\{^1\text{H}\}$ NMR (125.8 MHz, CD_2Cl_2): δ = 207.3 (br; C^1), 199.7 (d, $J(\text{P,C})$ = 23.7 Hz; C^4), 157.3 and 138.2 (s; C^7 and C^6), 126.0 (d, $J(\text{P,C})$ = 27.0 Hz; C^3), 116.1 (d, $J(\text{P,C})$ = 72.5 Hz; C^2), 116.1–157.4 (m; Ph), 49.9 ppm (s; C^5); HRMS (ESI): m/z calcd for $\text{C}_{61}\text{H}_{47}\text{N}_2\text{S}_2\text{P}_3\text{Os}$: 1156.2008 [M] $^+$; found: 1156.1996.

Synthesis of [(SCN) $_2$ (PPh $_3$) $_2$ Os{CHC(PPh $_3$)CHCHC(NH*n*Bu)}] (6): A suspension of sodium methoxide (59 mg, 1.1 mmol) in MeOH (1 mL, 24.71 mmol) was added to a solution of compound **2** (260 mg, 0.20 mmol) in CH_2Cl_2 (10 mL). The mixture was stirred at RT for about 1 min and then *n*-butylamine (0.20 mL, 2.0 mmol) was added. The mixture was stirred for a further 30 min to give a deep-green suspension. The solvent was removed under vacuum and the residue was extracted with CH_2Cl_2 (3 \times 2 mL). The volume of the filtrate was concentrated to about 2 mL under vacuum. Et_2O (20 mL) was slowly added with stirring to give a deep-green precipitate and a yellow-green solution, which were separated by filtration. The solvent of the yellow-green filtrate was removed under vacuum, which produced a green solid that was collected by filtration and washed with *n*-hexane (3 \times 2 mL). Yield: 87 mg, 35%. As indicated by in situ NMR spectroscopy, compounds **6** (Yield (by NMR spectroscopy): 40%) and **8** (Yield (by NMR spectroscopy): 60%) were both contained in the deep-green solution. Disappointingly, our attempts to isolate compound **8** were not successful. ^1H NMR (400.1 MHz, CDCl_3): δ = 15.2 (d, $J(\text{P,H})$ = 23.6 Hz, 1H; C^1H), 6.8 (t, $J(\text{P,H})$ = 10.1 Hz, $J(\text{H,H})$ = 10.1 Hz, 1H; C^3H), obscured by the phenyl signals but confirmed by $^1\text{H},^{13}\text{C}$ HMQC experiments), 6.6–7.7 ppm (m, 46H; Ph and *NH*), 5.4 (d, $J(\text{P,H})$ = 10.1 Hz, 1H; C^4H), 2.0 (br, 2H; $\text{NHCH}_2\text{CH}_2\text{CH}_2\text{CH}_3$), 0.6 (m, 2H; $\text{NHCH}_2\text{CH}_2\text{CH}_2\text{CH}_3$), 0.9 (m, 2H; $\text{NHCH}_2\text{CH}_2\text{CH}_2\text{CH}_3$), 0.6 ppm (t, $J(\text{H,H})$ = 7.2 Hz, 3H; $\text{NHCH}_2\text{CH}_2\text{CH}_2\text{CH}_3$); $^{31}\text{P}\{^1\text{H}\}$ NMR (162.0 MHz, CDCl_3): δ = 16.9 (s; C^2PPh_3), 0.5 ppm (s; OsPPh_3); $^{13}\text{C}\{^1\text{H}\}$ NMR (125.8 MHz, CD_2Cl_2 , with $^1\text{H},^{13}\text{C}$ HSQC and ^{13}C dept-135 NMR experiments): δ = 212.7 (br; C^1), 229.7 (br; C^5), 143.4 (d, $J(\text{P,C})$ = 23.3 Hz; C^3), 142.7 and 137.6 (s; $\text{Os}(\text{NCS})_2$), 134.7–122.4 (m; Ph), 112.1 (d, $J(\text{P,C})$ = 12.3 Hz; C^4), 101.4 (d, $J(\text{P,C})$ = 78.5 Hz; C^2), 45.5 (s; $\text{NHCH}_2\text{CH}_2\text{CH}_2\text{CH}_3$), 30.9 (s; $\text{NHCH}_2\text{CH}_2\text{CH}_2\text{CH}_3$), 20.4 (s; $\text{NHCH}_2\text{CH}_2\text{CH}_2\text{CH}_3$), 14.2 ppm (s; $\text{NHCH}_2\text{CH}_2\text{CH}_2\text{CH}_3$); HRMS (ESI): m/z calcd for $\text{C}_{65}\text{H}_{58}\text{N}_3\text{S}_2\text{P}_3\text{Os}$: 1229.2900 [M] $^+$; found: 1229.2903.

Synthesis of [(SCN) $_2$ (PPh $_3$) $_2$ Os{CHC(PPh $_3$)CHCHC(NHPh)}] (7): A suspension of sodium methoxide (70 mg, 1.3 mmol) in MeOH (1.3 mL, 32.13 mmol) was added to a solution of compound **2** (280 mg, 0.22 mmol) in CH_2Cl_2 (10 mL). The mixture was stirred at RT for about 1 min, then aniline (0.21 mL, 2.3 mmol) was added. The mixture was stirred for a further 30 min to give a deep-green suspension. The solid suspension was removed by filtration and the volume of the filtrate was concentrated to about 2 mL under vacuum. The residue was purified by column chromatography on neutral alumina (acetone/ CH_2Cl_2 , 1:20) to give compound **7** as a green solid. Yield: 104 mg, 38%. As indicated by in situ NMR spectroscopy, compounds **7** (Yield (by NMR spectroscopy): 44%) and **9** (Yield (by NMR spectroscopy): 56%) were both contained in the deep-green reaction solution. Disappointingly, our attempts to isolate compound **9** were not successful. ^1H NMR (500.2 MHz, CD_2Cl_2): δ = 15.3 (d, $J(\text{P,H})$ = 23.4 Hz, 1H; C^1H), 9.1 (s, 3H; *NH*), 6.9 (t, $J(\text{P,H})$ = 10.3 Hz, $J(\text{H,H})$ = 10.3 Hz, 1H; C^3H), obscured by the phenyl signals but confirmed by $^1\text{H},^{13}\text{C}$ HMQC experiments), 6.2–7.8 ppm (m, 50H; Ph), 6.0 ppm (d, $J(\text{P,H})$ = 10.3 Hz, 1H; C^4H). $^{31}\text{P}\{^1\text{H}\}$ NMR (202.5 MHz, CD_2Cl_2): δ = 16.7 ppm (s; C^2PPh_3), –1.4 (s; OsPPh_3); $^{13}\text{C}\{^1\text{H}\}$ NMR (125.8 MHz, CD_2Cl_2 , with $^1\text{H},^{13}\text{C}$ HSQC and ^{13}C dept-135 NMR experiments): δ = 217.3 (br; C^1), 228.9 (br; C^5), 143.2 (d, $J(\text{P,C})$ = 22.8 Hz; C^3), 143.6 and 139.4 (s; $\text{Os}(\text{NCS})_2$), 140.7–118.8 (m; Ph), 115.2 (d, $J(\text{P,C})$ = 12.3 Hz; C^4),

102.4 ppm (d, $J(\text{P,C})=77.6$ Hz; C^2); HRMS (ESI): m/z calcd for $\text{C}_{67}\text{H}_{54}\text{N}_3\text{S}_2\text{P}_3\text{Os}$: 1249.2587 $[M]^+$; found: 1249.2572.

Synthesis of $[(\text{SCN})_2(\text{PPh}_3)_2\text{Os}\{\text{CHC}(\text{PPh}_3)\text{CHC}(\text{CHNHR})\}]$: In an NMR tube, the primary amine ($\text{R}'\text{NH}_2$, about 3 equiv) was added to a solution of compound **2** (9.0 mg, 7.0×10^3 mmol) in CD_2Cl_2 (0.4 mL), which afforded a color change from green to deep green. The reaction was complete after 5 min at RT and the NMR spectra were collected.

R = *n*Bu (8**):** Yield (by NMR spectroscopy): 100%; ^1H NMR (500.2 MHz, CD_2Cl_2): $\delta=13.3$ (d, $J(\text{P,H})=14.7$ Hz, 1H; C^1H), 6.5–7.4 ppm (m, 48H; Ph, NH, C^5H , and C^3H), 2.2 (br, 2H; $\text{NHCH}_2\text{CH}_2\text{CH}_2\text{CH}_3$), 0.5–1.0 ppm (m, 7H; $\text{NHCH}_2\text{CH}_2\text{CH}_2\text{CH}_3$); $^{31}\text{P}\{^1\text{H}\}$ NMR (202.5 MHz, CD_2Cl_2): $\delta=10.3$ (s; C^1P), -2.2 ppm (s; OsPPh_3). Disappointingly, the poor solubility of compound **8** prevented its $^{13}\text{C}\{^1\text{H}\}$ NMR characterization. HRMS (ESI): m/z calcd for $\text{C}_{65}\text{H}_{58}\text{N}_3\text{S}_2\text{P}_3\text{Os}$: 1229.2900 $[M]^+$; found: 1229.2903.

R = Ph (9**):** Yield (by NMR spectroscopy): 100%; ^1H NMR (500.2 MHz, CD_2Cl_2): $\delta=14.5$ (d, $J(\text{P,H})=15.3$ Hz, 1H; C^1H), 11.0 (d, $J(\text{H,H})=13.4$ Hz, 1H; NH), 9.2 (d, $J(\text{P,H})=13.4$ Hz, 1H; C^5H), 6.1–7.3 ppm (m, 51H; Ph and C^3H); $^{31}\text{P}\{^1\text{H}\}$ NMR (202.5 MHz, CD_2Cl_2): $\delta=10.7$ (s; C^1P), -3.1 ppm (s; OsPPh_3). Disappointingly, the poor solubility of compound **9** prevented its $^{13}\text{C}\{^1\text{H}\}$ NMR characterization. HRMS (ESI): m/z calcd for $\text{C}_{67}\text{H}_{54}\text{N}_3\text{S}_2\text{P}_3\text{Os}$: 1249.2587 $[M]^+$; found: 1249.2592.

Synthesis of $[(\text{SCN})_2(\text{PPh}_3)_2\text{Os}\{\text{CHC}(\text{PPh}_3)\text{CHC}(\text{CHN}i\text{Bu})\}]$ (10**):** $i\text{BuNH}_2$ (30 μL , 0.30 mmol) was added to a solution of compound **2** (115 mg, 0.09 mmol) in CH_2Cl_2 (5 mL). The reaction solution was stirred at RT for about 5 min under a nitrogen atmosphere, then under an oxygen atmosphere or in air for a further 50 min. The solvent was removed under vacuum and washed with n -hexane (3×2 mL). A paramagnetic complex was collected as a green solid. Yield: 102 mg, 91%; HRMS (ESI): m/z calcd for $\text{C}_{65}\text{H}_{57}\text{N}_3\text{S}_2\text{P}_3\text{Os}$: 1229.2900 $[M+H]^+$; found: 1229.2888.

Crystallographic analysis: Crystals of compounds **3**, **5**, and **10** that were suitable for X-ray diffraction were grown from their solutions in CH_2Cl_2 that were layered with n -hexane; crystals of compound **2** that were suitable for X-ray diffraction were grown from its solution in CHCl_3 that was layered with n -hexane. Selected crystals of compounds **2**, **3**, **5**, and **10** were mounted on top of a glass fiber and transferred into a cold stream of nitrogen. Single-crystal X-ray diffraction data were collected on an Oxford Gemini S Ultra CCD Area Detector or a Bruker Apex CCD area detector with graphite-monochromated $\text{MoK}\alpha$ radiation ($\lambda=0.71073$ Å) or $\text{CuK}\alpha$ radiation ($\lambda=1.54178$ Å). All of the data were corrected for absorption effects by using the multi-scan technique. The structures were solved by using direct methods, expanded by difference Fourier syntheses, and refined by using full-matrix least-squares on F^2 with the Bruker SHELXTL (Version 6.10) program package. Non-H atoms were refined anisotropically, unless otherwise stated. Hydrogen atoms were introduced at their geometric positions and refined as riding atoms, unless otherwise stated. For further details on the crystal data, data collection, and refinements, see Table 3.

Computational details: The molecular geometries of the reactants, intermediates, transition states, and products were optimized by using density functional theory (DFT) calculations with the hybrid Becke3LYP (B3LYP) method.^[9] The 6–31 g** basis set was used for the C, O, N, and H atoms, whilst the effective core potentials (ECPs) of Hay and Wadt with the double- ζ valance basis set (LanL2DZ)^[10] were chosen to describe the Os, S, P, and I atoms. In addition, polarization functions were added for Os ($\zeta_d=0.886$, $\zeta_f=0.266$, $\zeta_g=0.340$, $\zeta_h=0.421$).^[11] Frequency analyses were performed to obtain the zero-point energies (ZPE) and to identify all of the stationary point as minima (zero imaginary frequencies) or transition states (one imaginary frequency) on the potential-energy surfaces (PES). Intrinsic reaction coordinate (IRC) calculations were also calculated for the transition states to confirm that such structures indeed connected two relevant minima.^[12] To cut the computational cost, the Ph_3P group was modeled as PH_3 . All calculations were performed with the Gaussian 03 software package.^[13]

To consider the solvent effects, a continuum medium was employed for the single-point energy calculations of all of the optimized species, by using UAHF radii on the conductor-like polarizable continuum model

(CPCM).^[14] CH_2Cl_2 was used as the solvent, according to the experimental reaction conditions.

Acknowledgements

We thank the 973 Program (2012CB821600), the National Natural Science Foundation of China (20925208, 21174115, 21272193), the Research Grants Council of Hong Kong (HKUST603711), and the Mingang Postdoctoral Science Foundation of China.

- [1] a) H.-J. Arpe, *Industrial Organic Chemistry*, Wiley-VCH, Weinheim, **2010**; b) H.-G. Franck, J. W. Stadelhofer, *Industrial Aromatic Chemistry*, Springer-Verlag, Berlin and New York, **1987**; c) F. Effenberger, *Angew. Chem.* **1980**, *92*, 147; *Angew. Chem. Int. Ed. Engl.* **1980**, *19*, 151; d) D. E. Pearson, C. A. Buehler, *Synthesis* **1972**, 533.
- [2] For a review of *cine*-substitution reactions, see: J. Suwiński, K. Świerczek, *Tetrahedron* **2001**, *57*, 1639.
- [3] For recent reviews, see: a) M. Paneque, M. L. Poveda, N. Rendón, *Eur. J. Inorg. Chem.* **2011**, *19*; b) G. Jia, *Coord. Chem. Rev.* **2007**, *251*, 2167; c) J. R. Bleeker, *Acc. Chem. Res.* **2007**, *40*, 1035; d) L. J. Wright, *Dalton Trans.* **2006**, 1821; e) C. W. Landorf, M. M. Haley, *Angew. Chem.* **2006**, *118*, 4018; *Angew. Chem. Int. Ed.* **2006**, *45*, 3914; f) G. Jia, *Acc. Chem. Res.* **2004**, *37*, 479; <lit g> J. R. Bleeker, *Chem. Rev.* **2001**, *101*, 1205.
- [4] For $\text{S}_{\text{E}}\text{Ar}$ reactions of metalla-aromatic compounds, see: a) W. Y. Hung, B. Liu, W. Shou, T. B. Wen, C. Shi, H. H. Y. Sung, I. D. Williams, Z. Lin, G. Jia, *J. Am. Chem. Soc.* **2011**, *133*, 18350; b) G. R. Clark, P. M. Johns, W. R. Roper, T. Söhnel, L. J. Wright, *Organometallics* **2011**, *30*, 129; c) G. R. Clark, P. M. Johns, W. R. Roper, L. J. Wright, *Organometallics* **2008**, *27*, 451; d) T. B. Wen, S. M. Ng, W. Y. Hung, Z. Y. Zhou, M. F. Lo, L.-Y. Shek, I. D. Williams, Z. Lin, G. Jia, *J. Am. Chem. Soc.* **2003**, *125*, 884; e) C. E. F. Rickard, W. R. Roper, S. D. Woodgate, L. J. Wright, *Angew. Chem.* **2000**, *112*, 766; *Angew. Chem. Int. Ed.* **2000**, *39*, 750.
- [5] For $\text{S}_{\text{N}}\text{Ar}$ reactions of metalla-aromatic compounds, see: a) R. Lin, J. Zhao, H. Chen, H. Zhang, H. Xia, *Chem. Asian J.* **2012**, *7*, 1915; b) R. Lin, H. Zhang, S. Li, J. Wang, H. Xia, *Chem. Eur. J.* **2011**, *17*, 4223; c) H. Zhang, R. Lin, G. Hong, T. Wang, T. B. Wen, H. Xia, *Chem. Eur. J.* **2010**, *16*, 6999; d) G. R. Clark, L. A. Ferguson, A. E. McIntosh, T. Söhnel, L. J. Wright, *J. Am. Chem. Soc.* **2010**, *132*, 13443; e) T. Wang, S. Li, H. Zhang, R. Lin, F. Han, Y. Lin, T. B. Wen, H. Xia, *Angew. Chem.* **2009**, *121*, 6575; *Angew. Chem. Int. Ed.* **2009**, *48*, 6453; f) M. Paneque, C. M. Posadas, M. L. Poveda, N. Rendón, L. L. Santos, E. Álvarez, V. Salazar, K. Mereiter, E. Oñate, *Organometallics* **2007**, *26*, 3403; g) M. Paneque, C. M. Posadas, M. L. Poveda, N. Rendón, V. Salazar, E. Oñate, K. Mereiter, *J. Am. Chem. Soc.* **2003**, *125*, 9898.
- [6] a) T. Wang, H. Zhang, F. Han, R. Lin, Z. Lin, H. Xia, *Angew. Chem.* **2012**, *124*, 9976; *Angew. Chem. Int. Ed.* **2012**, *51*, 9838; b) Q. Zhao, L. Gong, C. Xu, J. Zhu, X. He, H. Xia, *Angew. Chem.* **2011**, *123*, 1390; *Angew. Chem. Int. Ed.* **2011**, *50*, 1354; c) R. Lin, H. Zhang, S. Li, L. Chen, W. Zhang, T. B. Wen, H. Zhang, H. Xia, *Chem. Eur. J.* **2011**, *17*, 2420; d) X. He, L. Gong, K. Kräling, K. Gründler, C. Frias, R. D. Webster, E. Meggers, A. Prokop, H. Xia, *ChemBioChem* **2010**, *11*, 1607; e) Y. Lin, H. Xu, L. Gong, T. B. Wen, X.-M. He, H. Xia, *Organometallics* **2010**, *29*, 2904; f) J. Huang, R. Lin, L. Wu, Q. Zhao, C. Zhu, T. B. Wen, H. Xia, *Organometallics* **2010**, *29*, 2916; g) H. Zhang, R. Lin, M. Luo, H. Xia, *Sci. China Chem.* **2010**, *53*, 1978; h) X.-M. He, Q. Liu, L. Gong, Y. Lin, T. B. Wen, *Inorg. Chem. Commun.* **2010**, *13*, 342; i) B. Liu, H. Wang, H. Xie, B. Zeng, J. Chen, J. Tao, T. B. Wen, Z. Cao, H. Xia, *Angew. Chem.* **2009**, *121*, 5538; *Angew. Chem. Int. Ed.* **2009**, *48*, 5430; j) B. Liu, H. Xie, H. Wang, L. Wu, Q. Zhao, J. Chen, T. B. Wen, Z. Cao, H. Xia, *Angew. Chem.* **2009**, *121*, 5569; *Angew. Chem. Int. Ed.* **2009**, *48*, 5461; k) H. Zhang, L. Wu, R. Lin, Q. Zhao, G. He, F. Yang, T. B. Wen, H. Xia, *Chem. Eur. J.* **2009**, *15*, 3546; l) L. Gong, Z. Chen, Y. Lin, X. He,

- T. B. Wen, X. Xu, H. Xia, *Chem. Eur. J.* **2009**, *15*, 6258; m) Y. Lin, L. Gong, H. Xu, X. He, T. B. Wen, H. Xia, *Organometallics* **2009**, *28*, 1524; n) L. Gong, Y. Lin, T. B. Wen, H. Xia, *Organometallics* **2009**, *28*, 1101; o) L. Wu, L. Feng, H. Zhang, Q. Liu, X. He, F. Yang, H. Xia, *J. Org. Chem.* **2008**, *73*, 2883; p) L. Gong, Y. Lin, T. B. Wen, H. Zhang, B. Zeng, H. Xia, *Organometallics* **2008**, *27*, 2584; q) L. Gong, Y. Lin, G. He, H. Zhang, H. Wang, T. B. Wen, H. Xia, *Organometallics* **2008**, *27*, 309; r) H. Zhang, L. Feng, L. Gong, L. Wu, G. He, T. B. Wen, F. Yang, H. Xia, *Organometallics* **2007**, *26*, 2705; s) H. Zhang, H. Xia, G. He, T. B. Wen, L. Gong, G. Jia, *Angew. Chem.* **2006**, *118*, 2986; *Angew. Chem. Int. Ed.* **2006**, *45*, 2920; t) H. Xia, G. He, H. Zhang, T. B. Wen, H. H. Y. Sung, I. D. Williams, G. Jia, *J. Am. Chem. Soc.* **2004**, *126*, 6862; u) G. He, H. Xia, G. Jia, *Chin. Sci. Bull.* **2004**, *49*, 1543.
- [7] a) K. C. Poon, L. Liu, T. Guo, J. Li, H. H. Y. Sung, I. D. Williams, Z. Lin, G. Jia, *Angew. Chem.* **2010**, *122*, 2819; *Angew. Chem. Int. Ed.* **2010**, *49*, 2759; b) P. M. Johns, W. R. Roper, S. D. Woodgate, L. J. Wright, *Organometallics* **2010**, *29*, 5358; c) A. F. Dalebrook, L. J. Wright, *Organometallics* **2009**, *28*, 5536; d) W. Y. Hung, J. Zhu, T. B. Wen, K. P. Yu, H. H. Y. Sung, I. D. Williams, Z. Lin, G. Jia, *J. Am. Chem. Soc.* **2006**, *128*, 13742; e) J. R. Bleeker, R. Behm, *J. Am. Chem. Soc.* **1997**, *119*, 8503.
- [8] a) E. Buncl, J. M. Dust, F. Terrier, *Chem. Rev.* **1995**, *95*, 2261; b) O. N. Chupakhin, V. N. Charushin, H. C. van der Plas, *Tetrahedron* **1988**, *44*, 1; c) H. C. van der Plas, M. Wozniak, H. J. W. van den Haak, *Adv. Heterocycl. Chem.* **1983**, *33*, 95; d) H. C. van der Plas, *Tetrahedron* **1985**, *41*, 237; e) H. C. van der Plas, *Acc. Chem. Res.* **1978**, *11*, 462.
- [9] a) A. D. Becke, *J. Chem. Phys.* **1993**, *98*, 1372; b) A. D. Becke, *J. Chem. Phys.* **1993**, *98*, 5648; c) A. D. Becke, *Phys. Rev. A* **1988**, *38*, 3098; d) C. Lee, W. Yang, R. G. Parr, *Phys. Rev. B* **1988**, *37*, 785.
- [10] a) C. E. Check, T. O. Faust, J. M. Bailey, B. J. Wright, T. M. Gilbert, L. S. Sunderlin, *J. Phys. Chem. A* **2001**, *105*, 8111; b) P. J. Hay, W. R. J. Wadt, *Chem. Phys.* **1985**, *82*, 299.
- [11] S. Huzinaga, *Gaussian Basis Sets for Molecular Calculations*, Elsevier, Amsterdam, **1984**.
- [12] a) K. Fukui, *J. Phys. Chem.* **1970**, *74*, 4161; b) K. Fukui, *Acc. Chem. Res.* **1981**, *14*, 363.
- [13] Gaussian 03, revision B05, M. J. Frisch, G. W. Trucks, H. B. Schlegel, G. E. Scuseria, M. A. Robb, J. R. Cheeseman, J. A. Montgomery, T., Jr., Vreven, K. N. Kudin, J. C. Burant, J. M. Millam, S. S. Iyengar, J. Tomasi, V. Barone, B. Mennucci, M. Cossi, G. Scalmani, N. Rega, G. A. Petersson, H. Nakatsuji, M. Hada, M. Ehara, K. Toyota, R. Fukuda, J. Hasegawa, M. Ishida, T. Nakajima, Y. Honda, O. Kitao, H. Nakai, M. Klene, X. Li, J. E. Knox, H. P. Hratchian, J. B. Cross, C. Adamo, J. Jaramillo, R. Gomperts, R. E. Stratmann, O. Yazyev, A. J. Austin, R. Cammi, C. Pomelli, J. W. Ochterski, P. Y. Ayala, K. Morokuma, G. A. Voth, P. Salvador, J. J. Dannenberg, V. G. Zakrzewski, S. Dapprich, A. D. Daniels, M. C. Strain, O. Farkas, D. K. Malick, A. D. Rabuck, K. Raghavachari, J. B. Foresman, J. V. Ortiz, Q. Cui, A. G. Baboul, S. Clifford, J. Cioslowski, B. B. Stefanov, G. Liu, A. Liashenko, P. Piskorz, I. Komaromi, R. L. Martin, D. J. Fox, T. Keith, M. A. Al-Laham, C. Y. Peng, A. Nanayakkara, M. Challacombe, P. M. W. Gill, B. Johnson, W. Chen, M. W. Wong, C. Gonzalez, J. A. Pople, Gaussian, Inc., Pittsburgh PA, **2003**.
- [14] a) M. Cossi, N. Rega, G. Scalmani, V. Barone, *J. Comput. Chem.* **2003**, *24*, 669; b) V. Barone, M. Cossi, *J. Phys. Chem. A* **1998**, *102*, 1995.

Received: April 12, 2013
Published online: July 10, 2013